# Computational and experimental studies of reactive intermediates in glycosylation reactions

Remmerswaal, W.A.

# Chapter 4

## Neighboring-group Participation by C-2 Acyloxy Groups: Influence of the Nucleophile and Acyl Group on the Stereochemical Outcome of Acetal Substitution Reactions

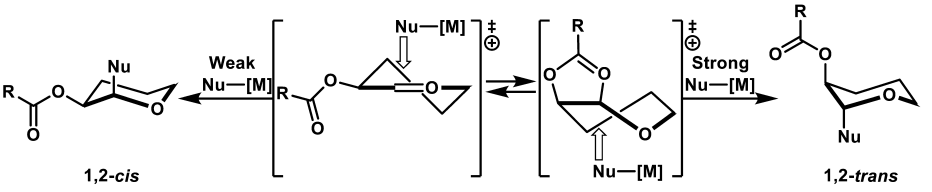


R = Me, *p*-OMe-$C_6H_4$, Ph, *p*-$NO_2$-$C_6H_4$

Abstract | A single acyloxy group at C-2 can control the outcome of nucleophilic substitution reactions of pyran-derived acetals, but the extent of the neighboring-group participation depends on a number of factors. It is shown here that neighboring-group participation does not necessarily control the stereochemical outcome of acetal substitution reactions with weak nucleophiles. The 1,2-*trans* selectivity increased with increasing reactivity of the incoming nucleophile. This trend suggests the intermediacy of both *cis*-fused dioxolenium ions and oxocarbenium ions in the stereochemistry-determining step. In addition, as the electron-donating ability of the neighboring group decreased, the preference for the 1,2-*trans* products increased. Computational studies show how the barriers for the ring-opening reaction on the dioxolenium ions and the transition states to provide the oxocarbenium ions change with the electron-donating capacity of the C-2-acyloxy group and the reactivity of the nucleophile.

Published | Chun, Y.; Remmerswaal, W. A.; Codée, J. D. C.; Woerpel, K. A. *Chem. Eur. J.* **2023**, 29, e202301894.

# Introduction

Neighboring-group participation involving acyloxy groups is an effective strategy to control stereoselectivity in substitution reactions of acetals and glycosylation reactions, allowing for the synthesis of a range of biologically relevant compounds.[1–5] Upon activation of an acetal an oxocarbenium ion (**1**) is formed, then a C-2-acyloxy group can interact with the anomeric center to form a stabilized *cis*-fused dioxolenium ion resembling **2** (Scheme 1), which can be opened by a nucleophile to form the 1,2-*trans* product stereoselectively.[5–12] Although neighboring-group participation can be a powerful means to exert stereocontrol in acetal substitution reactions and has become one of the cornerstones of carbohydrate chemistry, the presence of a neighboring acyloxy group does not assure high selectivity.[1,3,5,13–15] Understanding the factors that contribute to the success or failure of an acyloxy group to control stereoselectivity in glycosylation reactions can be challenging considering that other, more remote substituents on glycosyl donors can also exert considerable influence on the stereochemical outcomes of acetal substitution reactions.[16–20] It is therefore difficult to derive general principles to guide the use of neighboring groups to control the stereochemical courses of nucleophilic substitution reactions of acetals.

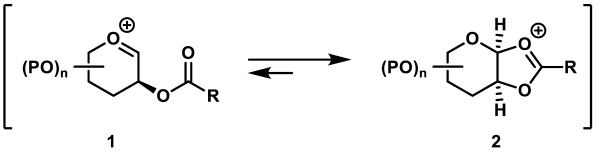


**Scheme 1**. Oxocarbenium ion **1** converts to the stabilized cis-fused dioxolenium ion **2**.

By examining reactions of acetals carrying a single C-2-acyloxy group, it is demonstrated how sensitive neighboring-group participation is to the nature of the acyloxy group at C-2 as well as to the reactivity of the incoming nucleophile. Substitutions of acetals bearing C-2 acyloxy groups with strong nucleophiles are generally highly 1,2-*trans* diastereoselective, but selectivity decreases as nucleophilicity decreases, in violation of the reactivity-selectivity principle.[21] This trend is consistent with two reaction pathways involving two different reactive intermediates: the more stabilized *cis* dioxolenium ions can form the 1,2-*trans* products through a ring-opening substitution reaction by a strong nucleophile, while weak nucleophiles react with the more reactive oxocarbenium ions, leading to mixtures of products. The extent of stereochemical control depends on the electronic nature of the neighboring group. Reactions of weaker nucleophiles can be rendered highly 1,2-*trans* selective by use of a participating group that is less electron-donating,[22–25] allowing the reaction to proceed through a less stabilized, more reactive *cis*-fused dioxolenium ion.

## Results and Discussion

The investigation was started by studying the substitution of acetal **3**, carrying a C-2-acetoxy group, using allyltrimethylsilane as a small nucleophile that reacts irreversibly with carbocations.[26–29] In this reaction, the inability of the single acetoxy group to deliver 1,2-*trans* selectivity immediately became apparent (Table 1). Instead of formation of the expected products, the 1,2-*cis* products were observed.[30] Changing the nucleophilicity of the acceptor had a drastic effect on the extent of stereocontrol exerted by the single C-2-acyloxy group (Table 1). The two weakest nucleophiles, allylchlorodimethylsilane and allyltrimethylsilane, reacted with the same diastereoselectivity (Table 1, entry 1 and 2), which is similar to that for allylation of the C-2-benzyloxy-substituted acetal.[16] The similar diastereoselectivities likely reflects the intrinsic selectivity of reactions involving an oxocarbenium ion. With increasing nucleophilicity, as measured by the nucleophilicity parameter *N*,[28,31,32] the relative amount of the 1,2-*trans* product increased. The 1,2-*trans* product *trans*-**7** was formed as a single diastereomer in the substitution with sterically hindered silyl ketene acetal **13** (entry 6). A dioxolane product **14** was also isolated in 15% yield (Scheme 2), providing evidence for the formation of the *cis* dioxolenium ion (*i.e.*, **2**).[33] Steric interactions may contribute to the high diastereoselectivity in the formation of products *trans*-**7** and **14** considering the steric bulk of the nucleophile **13**.

**Table 1.** Nucleophilic substitution reactions of acetal **3** with *C*-nucleophiles.[a,b,c]

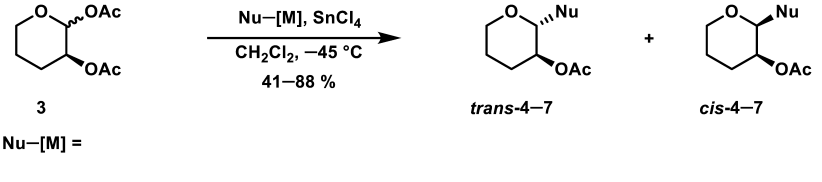


| Entry | Nu–[M] | *N* Number[d] | Product | *trans*:*cis* | (yield) |
|---|---|---|---|---|---|
| 1 | **8** | –0.6 | **4** | 23:77 | ( – %)[e] |
| 2 | **9** | 1.7 | **4** | 23:77 | (68%) |
| 3 | **10** | 4.4 | **5** | 48:52 | (68%) |
| 4[f] | **11** | 5.5 | **4** | 55:45 | (31%) |
| 5 | **12** | 6.2 | **6** | 83:17 | (74%) |
| 6[g] | **13** | 9.0 | **7** | ≥ 99:1 | (56%) |

[a] Diastereomeric ratios were determined by $^{13}C$ NMR spectroscopy analysis of the unpurified reaction mixtures.[30,34] [b] Acetal **3** was used as a mixture of diastereomers. The anomer ratio of the starting material should not exert influence on the diastereomeric ratios. [c] Attempts to use stronger silyl ketene acetal nucleophiles failed due to decomposition of the nucleophile under various reaction conditions. [d] Higher *N* numbers correlate to higher nucleophilicities.[31,32] [e] The spectral data obtained were consistent with those of products from entry 1. [f] $BF_3$•$OEt_2$ used as the activator.[15] [g] *N* number estimated with the corresponding $Me_3Si$-protected silyl ketene acetal.[31,32]

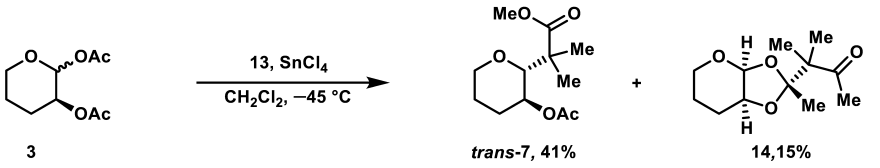


**Scheme 2.** Substitutions of acetal **3** with silyl ketene acetal **13**

The stereoselectivity trends observed for the substitutions suggest that both *cis*-fused dioxolenium ions and oxocarbenium ions can be involved in the stereochemistry-determining step (Scheme 3). Formation of dioxolane product **14** provided evidence for the involvement of dioxolenium ions (*i.e.*, **16**, Scheme 3).[33] Strong nucleophiles can attack these more stabilized and therefore less electrophilic dioxolenium ions on the face opposite to the acyloxy group, leading to the formation of 1,2-*trans* products.[35] In contrast, the formation of the 1,2-*cis* products originates from attack of the oxocarbenium ions by the weaker nucleophiles (*i.e.*, **15**, Scheme 3).[16,17,36] Reactions that provide significant quantities of both products could arise from a combination of these two pathways, or from reactions of the oxocarbenium ion **15** with a nucleophile at rates approaching the rate of diffusion, which would lead to both stereoisomers of product.[37–39]

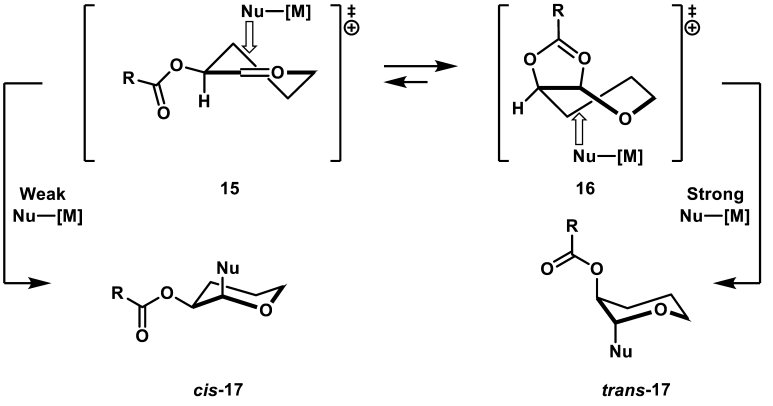


**Scheme 3.** Nucleophilic additions to oxocarbenium ion **15** and *cis* dioxolenium ion **16**.

It can be reasoned that the relative importance of the two pathways depicted in Scheme 3 could depend upon the electron-donating ability of the neighboring group,[40,41] and so the reactions of acetals with different C-2-benzoyloxy groups (Table 2) were investigated. The reactions of benzoates **18**-**20** with nucleophiles **9**-**11** followed a general trend that was unanticipated: the amount of 1,2-*trans* product increased with decreasing electron-donating capacity along the series *p*-MeO-$C_6H_4$ ≈ Ph < *p*-$NO_2$-$C_6H_4$. Considering that the 1,2-*cis* product must arise from the oxocarbenium ion, the trends show that the dioxolenium ions formed from the weaker participating groups are more readily displaced by the nucleophiles. This trend suggests that the transition states for ring-opening of the dioxolenium ion involve considerable bond breaking (see below).[5,13]

**Table 2.** Substitutions of benzoates **18**–**20** with *C*-nucleophiles.[a,b]

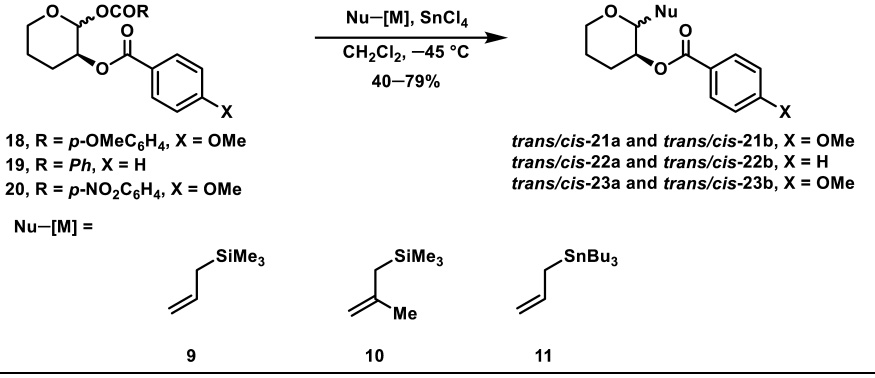


| Entry | Nu–[M] | N Number[c] | Product | *trans*:*cis* (X = OMe) | *trans*:*cis* (X = H) | *trans*:*cis* (X = $NO_2$) |
|---|---|---|---|---|---|---|
| 1 | **9** | 1.7 | **21**–**23a** | 33:67 (51%) | 34:66 (40%) | 41:59 (46%) |
| 2 | **10** | 4.4 | **21**–**23b** | 52:48 (71%) | 55:45 (43%) | 84:16 (62%) |
| 3[d] | **11** | 5.5 | **21**–**23a** | 54:46 (–%)[e] | 62:38 (–%)[e] | 68:32 (–%)[e] |

[a] Diastereomeric ratios were determined by $^{13}C$ NMR spectroscopy analysis of the unpurified reaction mixtures. [30,34] [b] Acetals **18**, **19** and **20** were used as a mixture of diastereomers. The anomer ratio of the starting material should not exert influence on the diastereomeric ratios. [c] Higher *N* numbers correlate to higher nucleophilicities.[31,32] [d] $BF_3$•$OEt_2$ used as the activator.[42,43] Reactions warmed to 25 °C for efficient activation of the acetal leaving group. [e] The spectral data obtained were consistent with those of products from entry 1.

To provide insight into the general trends in diastereoselectivity as a function of the nature of the acyloxy group and the reactivity of the nucleophile, the substitution reactions were also studied computationally. All computations were performed with ORCA5.03[44–46] at the SMD(dichloromethane)-revDSD-PBEP86-D4-def2TZVPP//PCM(dichloromethane)-B3LYP-D3BJ-def2TZVPP[47–56] level of theory, which should provide an accurate assessment of the energy of oxocarbenium ions.[57] The first step involved establishing the conformational energy landscape[18,58,59] of the dioxolenium (**R**$_{\mathbf{Diox}}$) and oxocarbenium ions (**R**$_{3H4}$ and **R**$_{4H3}$) for the four aryl-substituted pyrans **24** (2-*O*-acetyl), **25** (2-*O*-*p*-methoxybenzoyl), **26** (2-*O*-benzoyl) and **27** (2-*O*-*p*-nitrobenzoyl) (Supporting Figure S1). In all cases, the dioxolenium ions, adopting a $^1S_3/B_{3,0}$ conformation, were significantly favored over their oxocarbenium ion counterparts, which preferentially adopted a $^3H_4$ structure.[5] As the electron-donating nature of the acyloxy group decreased,[22–25] the dioxolenium ion became less favored. The $O_1$–$C_1$ bond length of the dioxolenium ion reflected the stabilization by the acyloxy group: the *p*-nitrobenzoyloxy group coordinated less tightly to the cationic anomeric center, as reflected in its shorter $O_1$–$C_1$ and longer $O_2$–$C_1$ bonds compared to those for the other benzoyloxy groups (Table 3).

**Table 3**. Ground-state conformations of *cis*-fused dioxolenium ions **25**–**27**.[a]

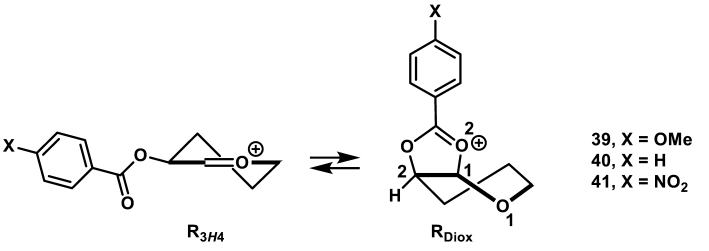


| Cation | Relative Energy, $\mathbf{R}_{3H4}$ / $\mathbf{R}_{Diox}$ ($\Delta G$, kcal mol$^{-1}$) | Bond length (Å) $O_1$–$C_1$ | Bond length (Å) $O_2$–$C_1$ |
|---|---|---|---|
| **25** | –13.4 | 1.344 | 1.526 |
| **26** | –11.2 | 1.338 | 1.545 |
| **27** | –8.8 | 1.331 | 1.569 |

[a] Computed at SMD(dichloromethane)-revDSD-PBEP86-D4-def2TZVPP//PCM(dichloromethane)-B3LYP-D3BJ-def2TZVPP and expressed as relative Gibbs free energy (T=228.15 K) in kcal mol$^{-1}$.

Next, the nucleophilicity-stereoselectivity trends were explored. To get a clear picture how the reactivity of the allyl nucleophiles influences the diastereoselectivity of the reactions, calculations were performed with the carbon nucleophiles presented in Table 1 (for computational feasibility, some groups were replaced with electronically similar but smaller groups).

The computed reaction profiles for the C-2-acetoxy substrate **24** (the reaction profiles for cations **25**-**27** can be found in Supporting Figure S2-S4) show that two possible pathways are available for reactions with nucleophiles: direct substitution of the dioxolenium ions (right pathway in Figure 1a) or opening of the dioxolenium ion to give a mixture of oxocarbenium conformers and subsequent attack on this ion (left pathway in Figure 1). The highest barrier on the latter pathway is the transition state for the ring opening to give the oxocarbenium ion intermediates (**24**-$\mathbf{R}_{3H4}$ and **24**-$\mathbf{R}_{4H3}$). The $S_E2'$ additions to the oxocarbenium ion were determined to be barrierless for all nucleophiles (Supporting Figure S5-S10). This absence of a well-defined transition state structure is in contrast with the results of chapter 2 and 3, likely resulting from the electron-withdrawing acetate group activating the oxocarbenium ions. The activation energy for direct ring-opening of the dioxolenium ion (**24**-$\mathbf{R}_{Diox}$) by the incoming nucleophiles decreases with increasing nucleophilicity (*N* number, Table 1) of the *C*-nucleophiles. For the weaker nucleophiles (nucleophiles **8** and **9**), the reaction barrier for ring-opening of the dioxolenium ion (**24**-$\mathbf{TS}_A$ and **24**-$\mathbf{TS}_B$, respectively) was computed to be higher than the barrier for formation of the oxocarbenium ion (**24**-$\mathbf{TS}_F$), while the barriers for the opening of the dioxolenium ion by the stronger nucleophiles **10** and **11** (**24**-$\mathbf{TS}_C$ and **24**-$\mathbf{TS}_D$, **respectively**) were similar to the barrier for formation of the oxocarbenium ion. The computations show that substitution of the dioxolenium ion with nucleophile **12** (**24**-$\mathbf{TS}_E$) and **13** (Supporting Figure S11) were more favorable than the generation of the oxocarbenium ion. With increasing reactivity of the nucleophiles, the geometries of the transition states change, with the Nuc–$C_1$ distance becoming longer and the $O_2$–$C_1$ distance shortening, suggesting that the transition states are becoming earlier (atom numbering is shown in Table 3).

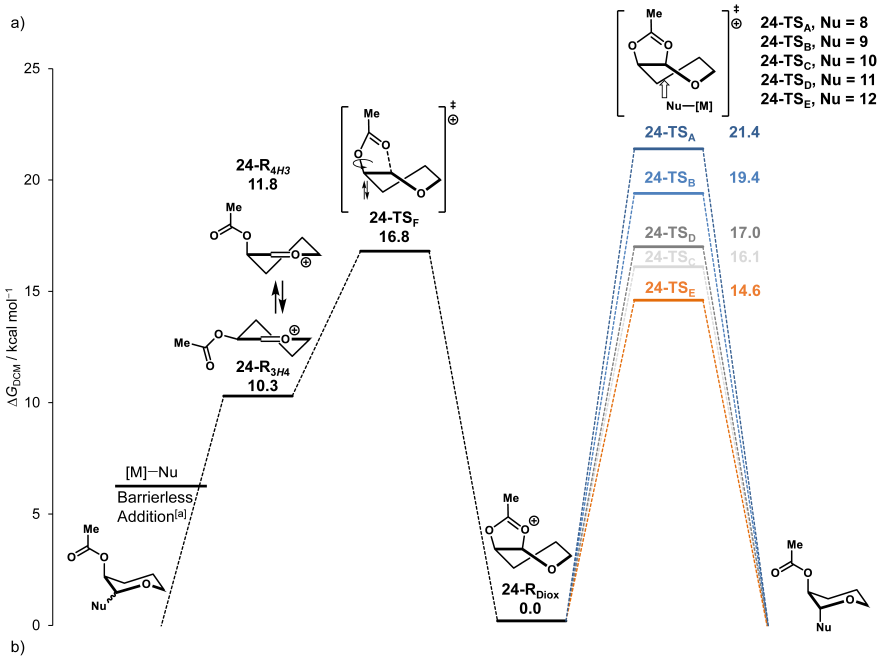


| Entry | Nu–[M] | dr (*trans*:*cis*) | **24–TS$_{A-E}$** (kcal mol$^{-1}$) | Relative Activation Energy, **24–TS$_{A-E}$** – **24–TS$_F$** ($\Delta\Delta G^{‡}$, kcal mol$^{-1}$) |
|---|---|---|---|---|
| 1 | **8** | 23:77 | 21.4 | +4.6 |
| 2 | **9** | 23:77 | 19.4 | +2.6 |
| 3 | **10** | 48:52 | 16.1 | –0.7 |
| 4[b] | **11** | 56:44 | 17.0 | –0.2 |
| 5[b] | **12** | 83:17 | 14.6 | –2.2 |
| 6[b] | **13** | ≥ 99:1 | [a] | [a] |

**Figure 1.** a) Reaction profiles of nucleophilic substitution reactions of 2-*O*-acetyl pyran cation **24** with *C*-nucleophiles **8** (**A**), **9** (**B**), **10** (**C**), **11** (**D**),[b] **12** (**E**). [b] b) Summary of critical substitution barrier heights compared to experimentally determined diastereomeric ratios.[30,34] Computed at SMD(dichloromethane)-revDSD-PBEP86-D4-def2TZVPP//PCM(dichloromethane)-B3LYP-D3BJ-def2TZVPP and expressed as relative Gibbs free energy (T=228.15 K) in kcal mol$^{-1}$. [a] Electronically barrierless, determined by constrained PES analysis. [b] The *t*-Bu groups of nucleophiles **11**, **12** were replaced with electronically similar but smaller methyl groups for computational feasibility.

Overall, the computed reaction profiles follow the observed reactivity-stereoselectivity trends and support the presence of two intermediates leading to products (Figure 1b). The computational studies also explain the correlation between the electron-donating capacity of the C-2 acyloxy group and the stereoselectivity of substitution reactions. The reaction profiles for the substitution of the aryl dioxolenium ions **25**-**27** with nucleophile **10** are depicted in Figure 2a.

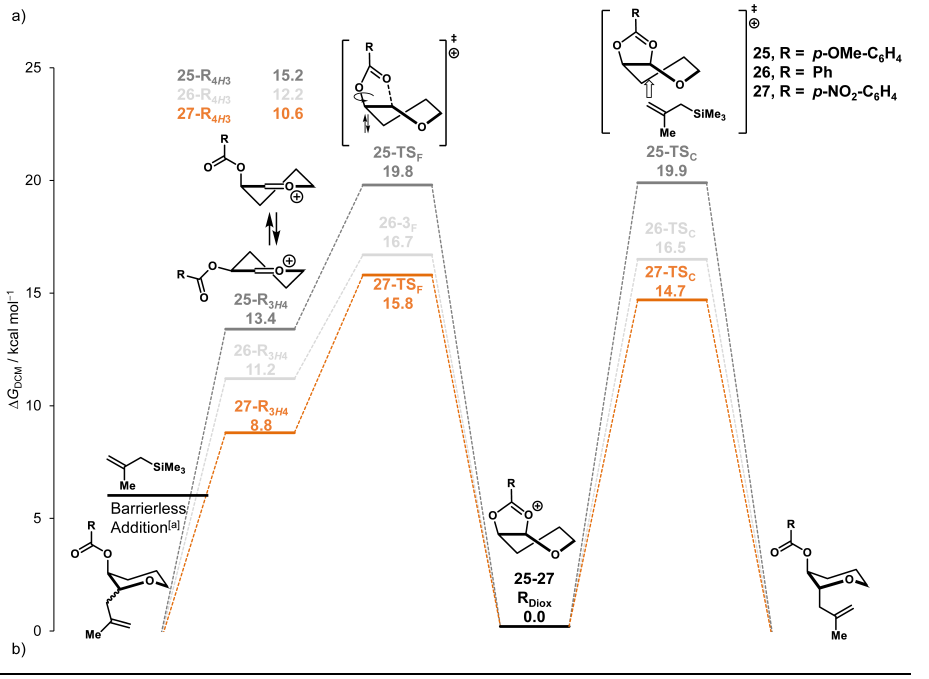


| Entry | R | dr (*trans*:*cis*) | **TS$_F$** (kcal mol$^{-1}$) | **TS$_C$** (kcal mol$^{-1}$) | Relative Activation Energy, **TS$_C$** – **TS$_F$** ($\Delta\Delta G^{‡}$, kcal mol$^{-1}$) |
|---|---|---|---|---|---|
| 1 | *p*-OMe-C$_6$H$_4$ (**25**) | 52:48 | 19.8 | 19.9 | +0.1 |
| 2 | Ph (**26**) | 55:45 | 16.7 | 16.5 | –0.2 |
| 3 | *p*-NO$_2$-C$_6$H$_4$ (**27**) | 84:16 | 15.8 | 14.7 | –1.1 |

**Figure 2.** a) Reaction profiles of nucleophilic substitution reactions of 2-*O*-aceloxy pyran cations (**25**, **26,** and **27**) with 2-methallyltrimehtylsilane (**10, C**). b) Summary of critical substitution barrier heights compared to experimentally found diastereomeric ratios.[30,34] Computed at SMD(dichloromethane)-revDSD-PBEP86-D4-def2TZVPP//PCM(dichloromethane)-B3LYP-D3BJ-def2TZVPP and expressed as relative Gibbs free energy (T=228.15 K) in kcal mol$^{-1}$. [a] Electronically barrierless, determined by constrained PES analysis.

The reaction profiles show minimal differences in barrier height between the ring-opening of the dioxolenium ion (right pathway, **25** and **26-TS$_C$**) and formation of the oxocarbenium ion (left pathway, **25** and **26-TS$_F$**) for both the *p*-methoxybenzoyloxy and benzoyloxy ions. By contrast, the transition state for the substitution reaction of the *p*-nitrobenzoyloxy group (**27-TS$_C$**) is lower in energy than the transition state leading to the oxocarbenium ion (**27-TS$_F$**) (Figure 2b). The net result is that the *p*-nitrophenyl dioxolenium ion **27** would form more product by the route involving the dioxolenium ion (the right pathway), leading to higher 1,2-*trans* stereoselectivity compared to the reactions of dioxolenium ions **25** and **26**. Examination of the transition state geometries for the substitution reactions show that the barrier height correlates with the $O_2$•••$C_1$ stretch (the elongation of the bond in the TS) of 1.06 Å, 1.03 Å, and 0.97 Å and a Nuc-$C_1$ distance of 2.38 Å, 2.42 Å, and 2.47 Å for **25**, **26**, and **27-TS$_C$**, respectively. This trend indicates a significantly earlier transition state for the nucleophilic attack on the *p*-nitrophenyl ion **27**.

When the related profiles for the weaker nucleophile **9** were generated (Supporting Figure S2-S4), the computations showed the substitution of the dioxolenium ions **25**-**27** by nucleophile **9** to be significantly higher ($\Delta\Delta G^{\ddagger}$∼+2—3 kcal mol$^{-1}$) than the barrier to form the oxocarbenium ions, explaining why changing the substituent on the benzoyl group has little effect on the stereoselectivity of these reactions because substitution on the dioxolenium ion is too unfavourable. Overall, the balance between the stabilization and reactivity of the dioxolenium ions and the reactivity of the incoming nucleophile determines the stereoselectivity of the acetal substitution reactions.

## Conclusions

In conclusion, the ability of acyloxy groups at C-2 of an acetal to guide the stereoselectivity of substitution reactions at the acetal carbon follows two general trends: 1) 1,2-*trans* selectivity increases with increased reactivity of the nucleophiles; and 2) 1,2-*trans* selectivity increases with decreased electron-donating ability of participating groups. Nucleophilic substitutions of acetals bearing common participating groups such as an acetate or a benzoate can be 1,2-*trans* diastereoselective for highly reactive nucleophiles, whereas reactions with weaker nucleophiles are generally unselective. To achieve 1,2-*trans* selectivity with less reactive nucleophiles, the installation of a less electron-donating acyloxy group, a group that might be regarded as a less powerful participating group, can lead to higher stereoselectivity because the resulting dioxolenium ion intermediate is less stabilized and therefore reacts more readily with weaker nucleophiles.

# Supporting information

**General computational methods**: All computations were performed with ORCA5.03[44–46] at SMD(dichloromethane)-revDSD-PBEP86-D4-def2TZVPP//PCM(dichloromethane)-B3LYP-D3BJ-def2TZVPP[47–56] level of theory. Geometries were optimized without symmetry constraints. All calculated stationary points have been verified by performing a vibrational analysis, to be energy minima (no imaginary frequencies) or transition states (only one imaginary frequency). The character of the normal mode associated with the imaginary frequency of the transition state has been analyzed with an intrinsic reaction coordinate (IRC) calculation to ensure that it is associated with the reaction of interest. When no clear transition state was found, constrained potential energy surface (PES) analysis was employed to verify the absence of a clear transition state.

**Constrained potential energy surface analysis**
To find transition states, the potential energy surface (PES) is scanned for a saddle point. Very simple bond cleavage events are often not associated with such a saddle point on the electronic energy surface, which makes it impossible to locate these transition states. To confirm this scenario for the $S_E2'$ reactions studied here, the elongation of the C-1•••Nucleophile bond (starting from the product complex) was examined. To this end the electronic relaxed potential energy surface was constructed. The starting point of each scan was the product complex. From here the C-1•••Nucleophile bond was elongated in 60 steps with a fine step size of 0.025Å, while allowing the rest of the geometry to optimize. A barrierless reaction was defined as the absence of a local maximum on this potential energy surface.

**Generation of the computational energy landscapes**
The workflow for the generation of computational energy landscapes (CEL) of pyranosyl[58] cations with ORCA5.03[44–46] was done similar to previous work.[27] Initial geometries were constructed by a highly constrained relaxed potential energy surface scan using the semi-empirical AM1 functional and the VerySlowConv keyword. All bond distances of directly connected atoms (*i.e.*, C1-H1 O5-C1, C2-O2, etc.) were constrained, as well as the H2-C2-O2-$O_{acyloxy}$ dihedral angle. The subsequent output geometries were then used as starting geometries for the CEL computations with constrains only on the C1-C2-C3-C4 and the C5-O5-C1-C2 dihedral angles. The C1-C2-C3-C4, C3-C4-C5-O5 and the C5-O5-C1-C2 dihedral angles were scanned from -60 to 60 degrees with 15 degree steps, generating 729 unique structures. The subsequent output geometries were then used as starting geometries for the CEL computations with constrains only on the C1-C2-C3-C4, C3-C4-C5-O5 and the C5-O5-C1-C2 dihedral angles. The CEL computations were then performed by optimization of the generated geometries, with constrains on the mentioned dihedral angles, with DFT using the keywords TightSCF, DEFGRID2 (optimization step), DEFGRID3 (single point step) and SlowConv at SMD(dichloromethane)-revDSD-PBEP86-D4-def2TZVPP//PCM(dichloromethane)-B3LYP-D3BJ-def2TZVPP.[47–56] The CEL maps were visualized using Origin 9.0.0[10] identical to Hansen *et al.*[58]

**Experimental methods**
Experimental results were generated by Yuge Chun. Synthetic procedures and details of stereochemical proofs can be found in the online supporting information of: Chun, Y.; Remmerswaal, W. A.; Codée, J. D. C.; Woerpel, K. A. Neighboring-Group Participation by C-2 Acyloxy Groups: Influence of the Nucleophile and Acyl Group on the Stereochemical Outcome of Acetal Substitution Reactions. *Chem. Eur. J.* **2023**, **29**, e202301894.[30,39]

**Supporting computational figures**

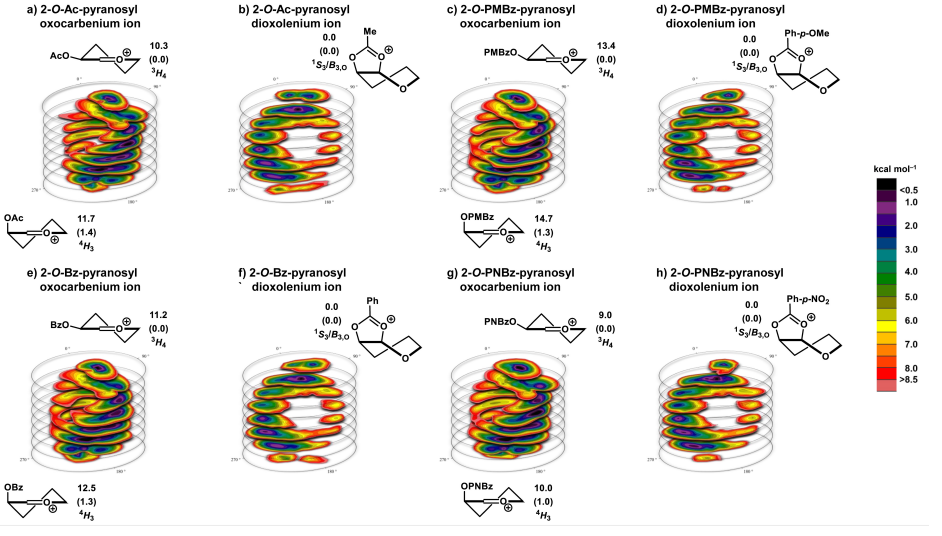


**Figure S1.** Conformational energy landscape (CEL) maps of 2-*O*-acetyl (Ac, **24**, a-b), 2-*O*-*p*-methoxybenzoyl (PMBz, **25**, c-d), 2-*O*-benzoyl (Bz, **26**, e-f) and 2-*O*-*p*-nitrobenzoyl (PNBz, **27**, g-h) pyran oxocarbenium and dioxolenium pyranosyl cations, in which the local minima identified are shown with their respective energy. Energies of all conformations in the CEL are computed at SMD(dichloromethane)-revDSD-PBEP86-D4-def2TZVPP//PCM(dichloromethane)-B3LYP-D3BJ-def2TZVPP and expressed as relative Gibbs free energy (T=228.15K) in kcal mol$^{-1}$. Energies given are relative to the dioxolenium ion. Between brackets, the energy relative between one CEL map is given.

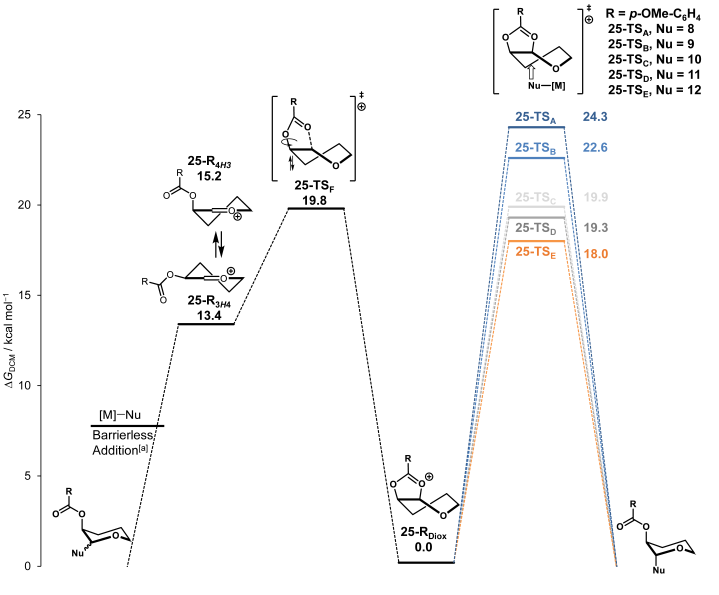


**Figure S2.** Reaction profiles of nucleophilic substitution reactions of 2-*O*-*p*-methoxybenzoyl pyran cations (**25**) with *C*-nucleophiles **8** (**A**), **9** (**B**), **10** (**C**), **11** (**D**),[b] **12** (**E**).[b] Computed at SMD(dichloromethane)-revDSD-PBEP86-D4-def2TZVPP//PCM(dichloromethane)-B3LYP-D3BJ-def2TZVPP and expressed as relative Gibbs free energy (T=228.15K) in kcal mol$^{-1}$. [a] Electronically barrierless, determined by constrained PES analysis. [b] The *t*-Bu groups of nucleophiles **11**, **12** were replaced with electronically similar but smaller methyl groups for computational feasibility.

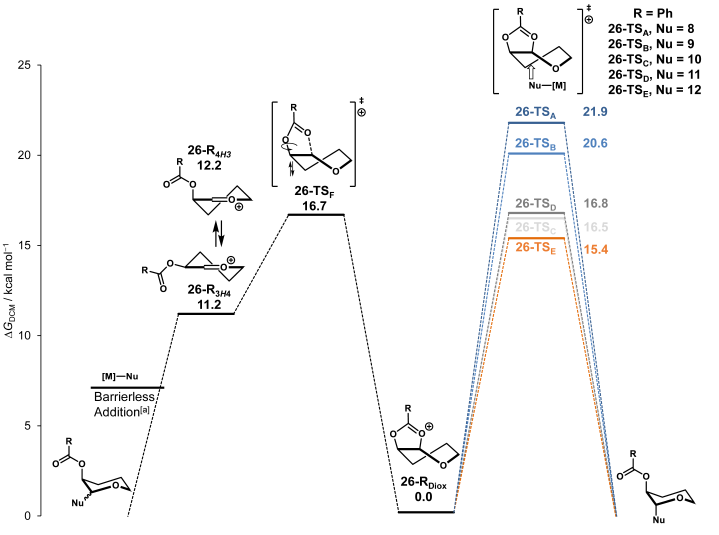


**Figure S3.** Reaction profiles of nucleophilic substitution reactions of 2-*O*-benzoyl pyran cations (**26**) with *C*-nucleophiles **8** (**A**), **9** (**B**), **10** (**C**), **11** (**D**),[b] **12** (**E**).[b] Computed at SMD(dichloromethane)-revDSD-PBEP86-D4-def2TZVPP//PCM(dichloromethane)-B3LYP-D3BJ-def2TZVPP and expressed as relative Gibbs free energy (T=228.15K) in kcal mol$^{-1}$. [a] Electronically barrierless, determined by constrained PES analysis. [b] The *t*-Bu groups of nucleophiles **11**, **12** were replaced with electronically similar but smaller methyl groups for computational feasibility.

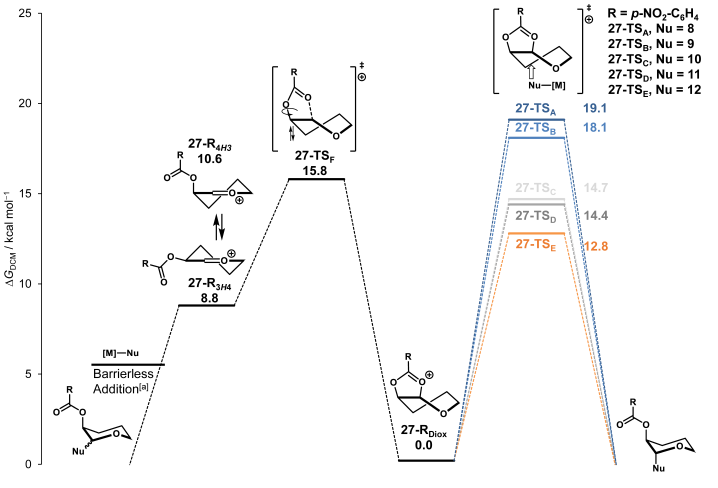


**Figure S4.** Reaction profiles of nucleophilic substitution reactions of 2-*O*-*p*-nitrobenzoyl pyran cations (**27**) with *C*-nucleophiles **8** (**A**), **9** (**B**), **10** (**C**), **11** (**D**),[b] **12** (**E**). [b] Computed at SMD(dichloromethane)-revDSD-PBEP86-D4-def2TZVPP//PCM(dichloromethane)-B3LYP-D3BJ-def2TZVPP and expressed as relative Gibbs free energy (T=228.15K) in kcal mol$^{-1}$. [a] Electronically barrierless, determined by constrained PES analysis. [b] The *t*-Bu groups of nucleophiles **11**, **12** were replaced with electronically similar but smaller methyl groups for computational feasibility.

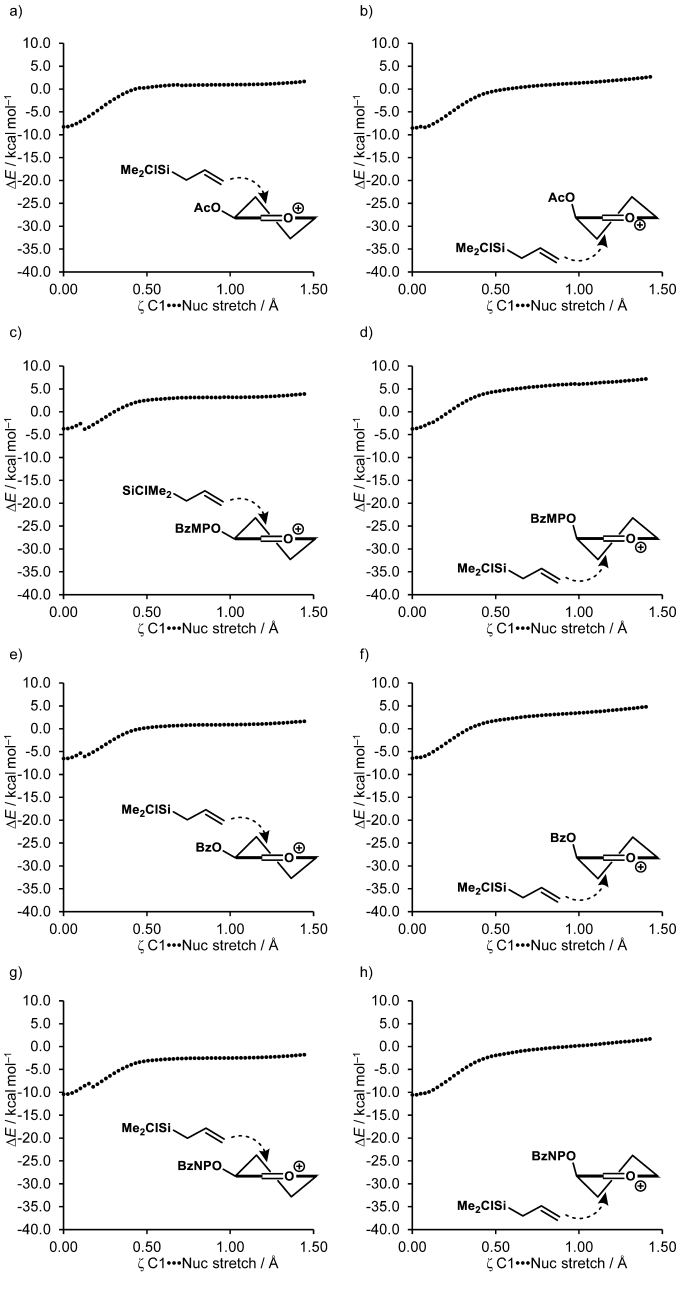


**Figure S5.** Constrained potential energy surface (PES) analysis of nucleophilic substitution reactions of 2-*O*-acetyl (Ac, **24**, a-b), 2-*O*-*p*-methoxybenzoyl (PMBz, **25**, c-d), 2-*O*-benzoyl (Bz, **26**, e-f) and 2-*O*-*p*-nitrobenzoyl (PNBz, **27**, g-h) pyran oxocarbenium cations ($\mathbf{R}_{3H4}$ and $\mathbf{R}_{4H3}$) with allyldimethylchlorosilane (step size = 0.025Å). Computed at PCM(dichloromethane)-B3LYP-D3BJ-def2TZVPP and expressed as electronic energy in kcal mol$^{-1}$.

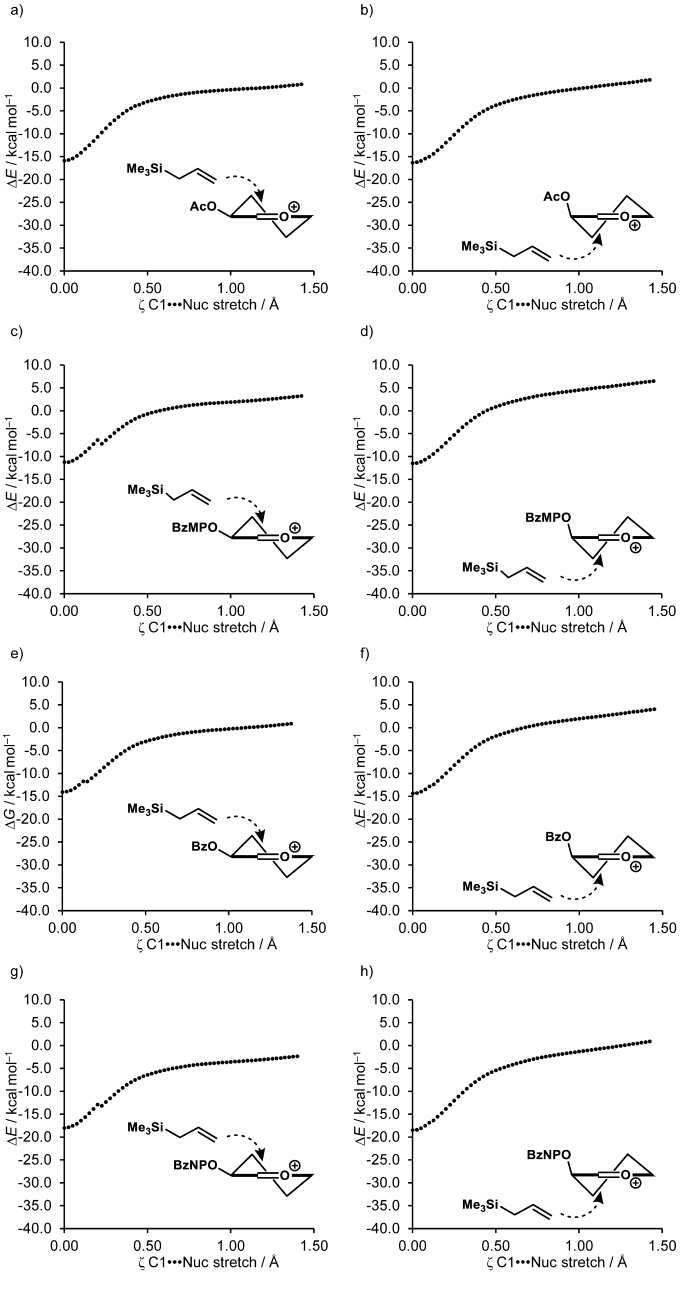


**Figure S6.** Constrained potential energy surface (PES) analysis of nucleophilic substitution reactions of 2-*O*-acetyl (Ac, **24**, a-b), 2-*O*-*p*-methoxybenzoyl (PMBz, **25**, c-d), 2-*O*-benzoyl (Bz, **26**, e-f) and 2-*O*-*p*-nitrobenzoyl (PNBz, **27**, g-h) pyran oxocarbenium cations (**$R_{3H4}$** and **$R_{4H3}$**) with allyltrimethylsilane (step size = 0.025Å). Computed at PCM(dichloromethane)-B3LYP-D3BJ-def2TZVPP and expressed as electronic energy in kcal mol$^{-1}$.

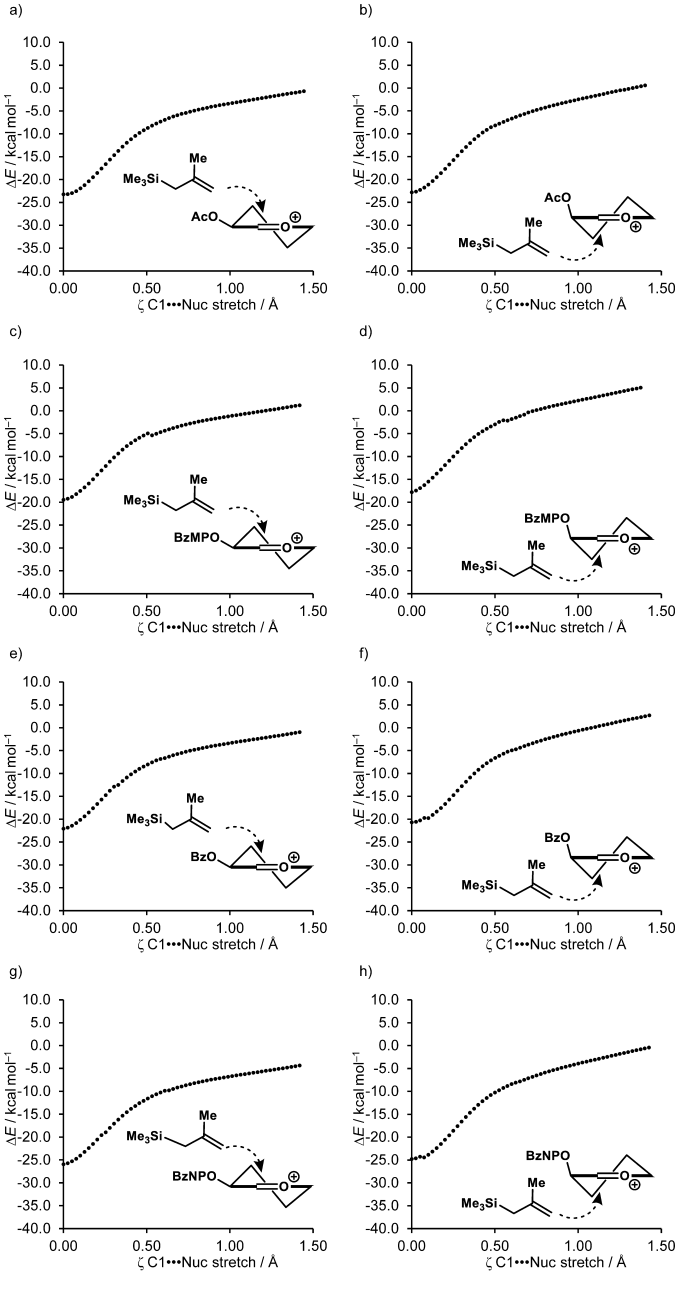


**Figure S7.** Constrained potential energy surface (PES) analysis of nucleophilic substitution reactions of 2-*O*-acetyl (Ac, **24**, a-b), 2-*O*-*p*-methoxybenzoyl (PMBz, **25**, c-d), 2-*O*-benzoyl (Bz, **26**, e-f) and 2-*O*-*p*-nitrobenzoyl (PNBz, **27**, g-h) pyran oxocarbenium cations (**R**$_{3H4}$ and **R**$_{4H3}$) with methallyltrimethylsilane (step size = 0.025Å). Computed at PCM(dichloromethane)-B3LYP-D3BJ-def2TZVPP and expressed as electronic energy in kcal mol$^{-1}$.

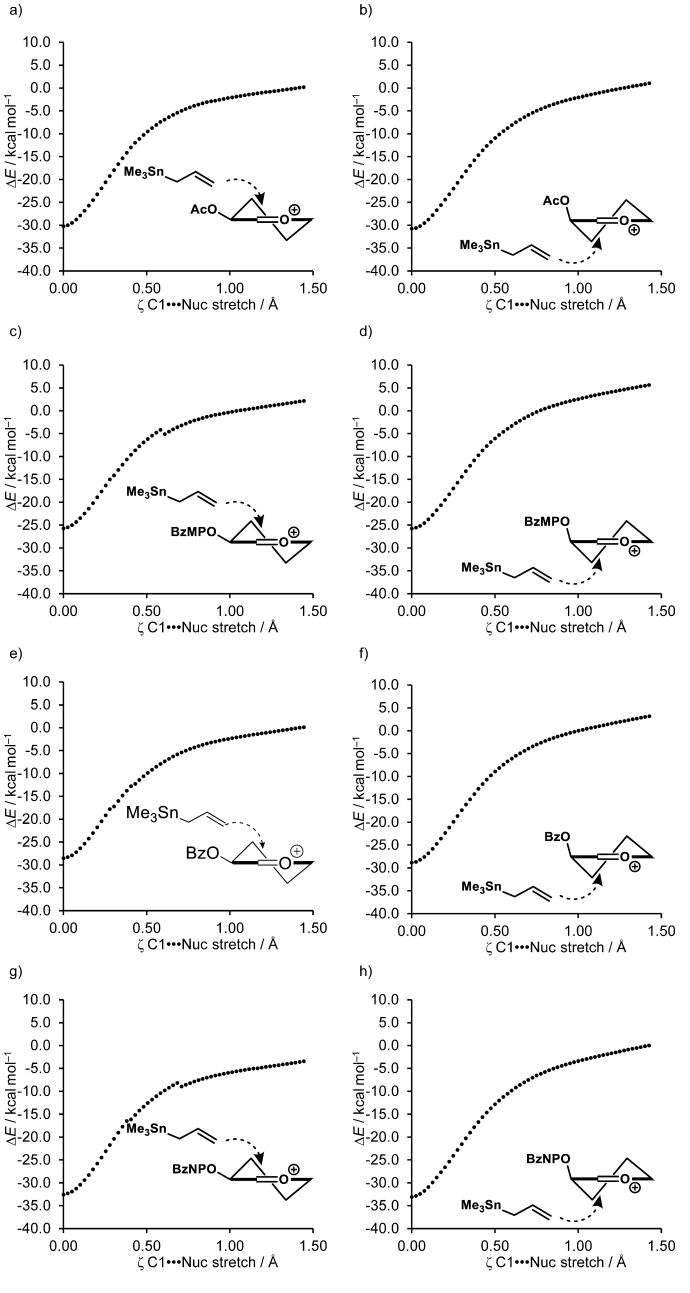


**Figure S8.** Constrained potential energy surface (PES) analysis of nucleophilic substitution reactions of 2-*O*-acetyl (Ac, **24**, a-b), 2-*O*-*p*-methoxybenzoyl (PMBz, **25**, c-d), 2-*O*-benzoyl (Bz, **26**, e-f) and 2-*O*-*p*-nitrobenzoyl (PNBz, **27**, g-h) oxocarbenium cations ($\mathbf{R}_{3H4}$ and $\mathbf{R}_{4H3}$) with allyltrimethylstannane (step size = 0.025Å). Computed at PCM(dichloromethane)-B3LYP-D3BJ-def2TZVPP and expressed as electronic energy in kcal mol$^{-1}$.

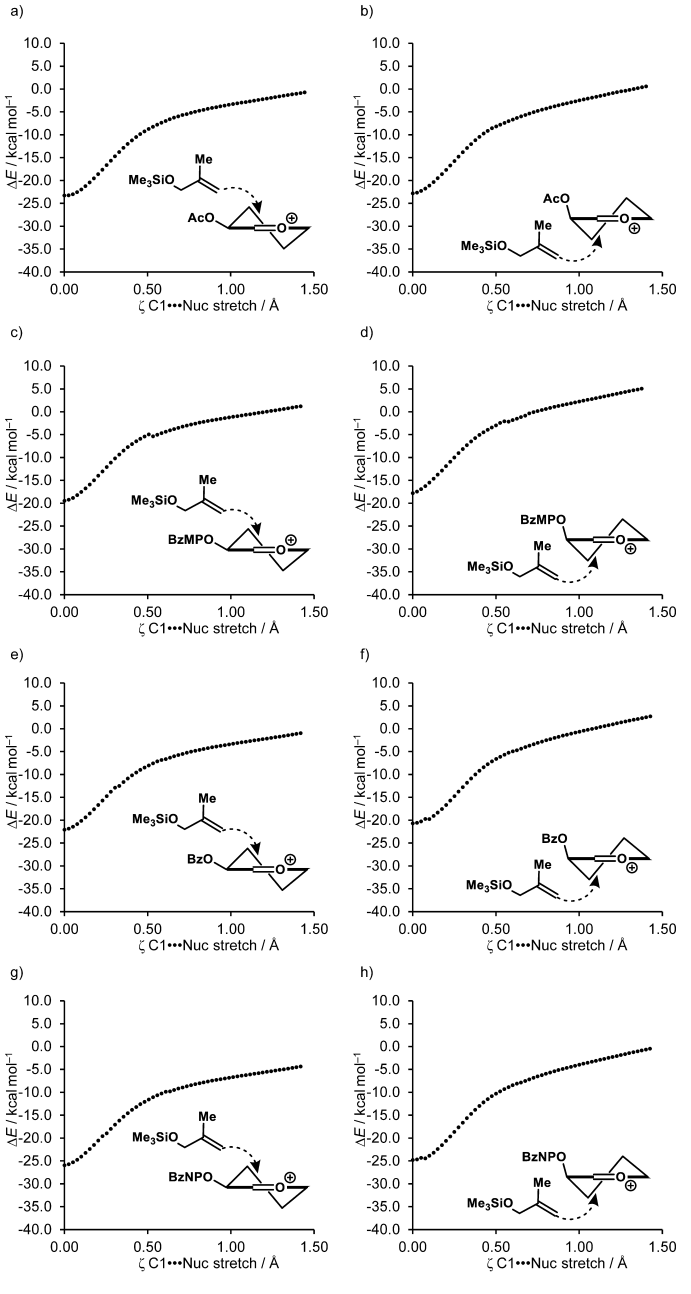


**Figure S9.** Constrained potential energy surface (PES) analysis of nucleophilic substitution reactions of 2-*O*-acetyl (Ac, **24**, a-b), 2-*O*-*p*-methoxybenzoyl (PMBz, **25**, c-d), 2-*O*-benzoyl (Bz, **26**, e-f) and 2-*O*-*p*-nitrobenzoyl (PNBz, **27**, g-h) pyran oxocarbenium cations (**R**$_{3H4}$ and **R**$_{4H3}$) with isopropenyloxytrimethylsilane (step size = 0.025Å). Computed at PCM(dichloromethane)-B3LYP-D3BJ-def2TZVPP and expressed as electronic energy in kcal mol$^{-1}$.

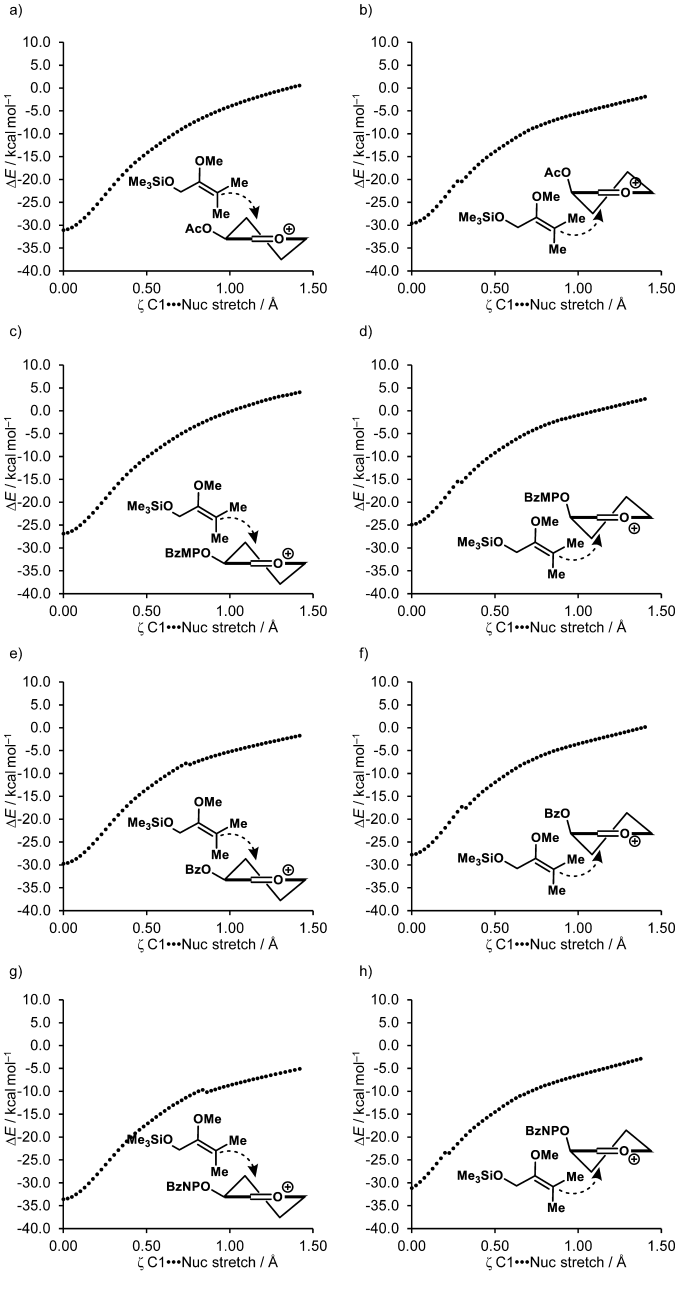


**Figure S10.** a) Constrained potential energy surface (PES) analysis of nucleophilic substitution reactions of 2-*O*-acetyl (Ac, **24**, a-b), 2-*O*-*p*-methoxybenzoyl (PMBz, **25**, c-d), 2-*O*-benzoyl (Bz, **26**, e-f) and 2-*O*-*p*-nitrobenzoyl (PNBz, **27**, g-h) pyran oxocarbenium cations ($\mathbf{R}_{3H4}$ and $\mathbf{R}_{4H3}$) with methyl trimethylsilyl dimethylketene acetal (step size = 0.025Å). Computed at PCM(dichloromethane)-B3LYP-D3BJ-def2TZVPP and expressed as electronic energy in kcal mol$^{-1}$.

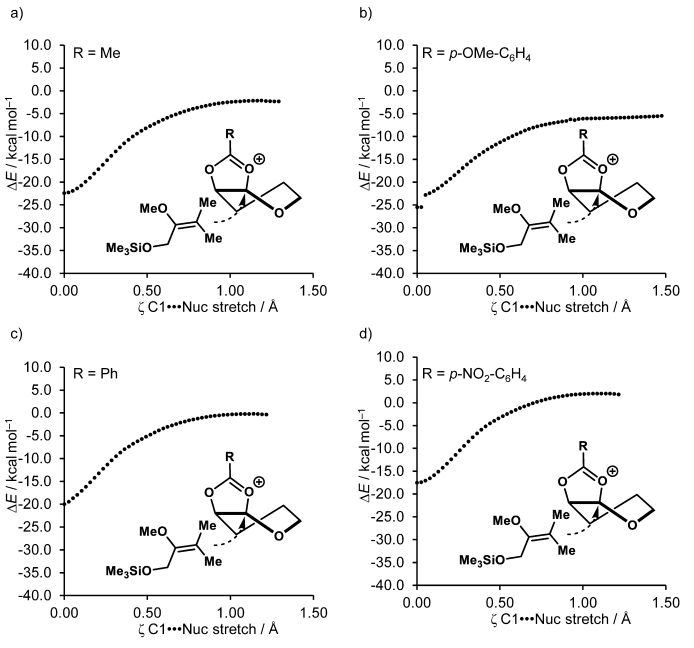


**Figure S11.** Constrained potential energy surface (PES) analysis of nucleophilic substitution reactions of 2-*O*-acetyl (Ac, **24**, a), 2-*O*-*p*-methoxybenzoyl (PMBz, **25**, b), 2-*O*-benzoyl (Bz, **26**, c) and 2-*O*-*p*-nitrobenzoyl (PNBz, **27**, d) pyran dioxolenium cations (**R**$_{\mathbf{Diox}}$) with methyl trimethylsilyl dimethylketene acetal (step size = 0.025Å). Computed at PCM(dichloromethane)-B3LYP-D3BJ-def2TZVPP and expressed as electronic energy in kcal mol$^{-1}$.

# References


(1) Ikeda, T.; Yamauchi, K.; Nakano, D.; Nakanishi, K.; Miyashita, H.; Ito, S.; Nohara, T. Chemical Trans-Glycosylation of Bioactive Glycolinkage: Synthesis of an α-Lycotetraosyl Cholesterol. *Tetrahedron Lett* **2006**, *47* (26), 4355–4359.

(2) Ohyama, K.; Okawa, A.; Moriuchi, Y.; Fujimoto, Y. Biosynthesis of Steroidal Alkaloids in Solanaceae Plants: Involvement of an Aldehyde Intermediate during C-26 Amination. *Phytochemistry* **2013**, *89*, 26–31.

(3) Williams, R. J.; McGill, N. W.; White, J. M.; Williams, S. J. Neighboring Group Participation in Glycosylation Reactions by 2,6-Disubstituted 2-*O*-Benzoyl Groups: A Mechanistic Investigation. *J. Carbohydr. Chem.* **2010**, *29* (5), 236–263.

(4) Bérces, A.; Enright, G.; Nukada, T.; Whitfield, D. M. The Conformational Origin of the Barrier to the Formation of Neighboring Group Assistance in Glycosylation Reactions: A Dynamical Density Functional Theory Study. *J. Am. Chem. Soc.* **2001**, *123* (23), 5460–5464.

(5) Nukada, T.; Berces, A.; Zgierski, M. Z.; Whitfield, D. M. Exploring the Mechanism of Neighboring Group Assisted Glycosylation Reactions. *J. Am. Chem. Soc.* **1998**, *120* (51), 13291–13295.

(6) Paulsen, H.; Trautwein, W.-P.; Espinosa, F. G.; Heyns, K. Carboxoniumverbindungen in der Kohlenhydratchemie, III. Einfache Synthese von D-Idose aus D-Glucose durch mehrfache Acetoxonium-Ion-Umlagerungen. Darstellung eines stabilen Acetoxonium-Salzes der Tetraacetyl-idose. *Chem. Ber.* **1967**, *100* (9), 2822–2836.

(7) Paulsen, H.; Herold, C.-P. Carboxoniumverbindungen in der Kohlenhydratchemie, X. Untersuchungen zur Acetoxonium-Umlagerung von D-Glucose zu D-Idose. *Chem. Ber.* **1970**, *103* (8), 2450–2462.

(8) Crich, D.; Dai, Z.; Gastaldi, S. On the Role of Neighboring Group Participation and Ortho Esters in β-Xylosylation: $^{13}C$ NMR Observation of a Bridging 2-Phenyl-1,3-Dioxalenium Ion. *J. Org. Chem.* **1999**, *64* (14), 5224–5229.

(9) Zeng, Y.; Wang, Z.; Whitfield, D.; Huang, X. Installation of Electron-Donating Protective Groups, a Strategy for Glycosylating Unreactive Thioglycosyl Acceptors Using the Preactivation-Based Glycosylation Method. *J. Org. Chem.* **2008**, *73* (20), 7952–7962.

(10) Nukada, T.; Berces, A.; Whitfield, D. M. Acyl Transfer as a Problematic Side Reaction in Polymer-Supported Oligosaccharide Synthesis. *J. Org. Chem.* **1999**, *64* (25), 9030–9045.

(11) Seeman, J. I. Effect of Conformational Change on Reactivity in Organic Chemistry. Evaluations, Applications, and Extensions of Curtin-Hammett Winstein-Holness Kinetics. *Chem. Rev.* **1983**, *83* (2), 83–134.

(12) Hettikankanamalage, A. A.; Lassfolk, R.; Ekholm, F. S.; Leino, R.; Crich, D. Mechanisms of Stereodirecting Participation and Ester Migration from Near and Far in Glycosylation and Related Reactions. *Chem. Rev.* **2020**, *120* (15), 7104–7151.

(13) Whitfield, D. M.; Nukada, T. DFT Studies of the Role of C-2–O-2 Bond Rotation in Neighboring-Group Glycosylation Reactions. *Carbohydr. Res.* **2007**, *342* (10), 1291–1304.

(14) Gade, M.; Paul, A.; Alex, C.; Choudhury, D.; Thulasiram, H. V.; Kikkeri, R. Supramolecular Scaffolds on Glass Slides as Sugar Based Rewritable Sensors for Bacteria. *Chem. Commun.* **2015**, *51* (29), 6346–6349.

(15) Mohamed, S.; He, Q. Q.; Lepage, R. J.; Krenske, E. H.; Ferro, V. Glycosylations of Simple Acceptors with 2-*O*-Acyl L-Idose or L-Iduronic Acid Donors Reveal Only a Minor Role for Neighbouring-Group Participation. *Eur. J. Org. Chem.* **2018**, *2018* (19), 2214–2227.

(16) Ayala, L.; Lucero, C. G.; Romero, J. A. C.; Tabacco, S. A.; Woerpel, K. A. Stereochemistry of Nucleophilic Substitution Reactions Depending upon Substituent: Evidence for Electrostatic Stabilization of Pseudoaxial Conformers of Oxocarbenium Ions by Heteroatom Substituents. *J. Am. Chem. Soc.* **2003**, *125* (50), 15521–15528.

(17) Romero, J. A. C.; Tabacco, S. A.; Woerpel, K. A. Stereochemical Reversal of Nucleophilic Substitution Reactions Depending upon Substituent: Reactions of Heteroatom-Substituted Six-Membered-Ring Oxocarbenium Ions through Pseudoaxial Conformers. *J. Am. Chem. Soc.* **2000**, *122* (1), 168–169.

(18) Hansen, T.; Elferink, H.; van Hengst, J. M. A.; Houthuijs, K. J.; Remmerswaal, W. A.; Kromm, A.; Berden, G.; van der Vorm, S.; Rijs, A. M.; Overkleeft, H. S.; Filippov, D. V.; Rutjes, F. P. J. T.; van der Marel, G. A.; Martens, J.; Oomens, J.; Codée, J. D. C.; Boltje, T. J. Characterization of Glycosyl Dioxolenium Ions and Their Role in Glycosylation Reactions. *Nat. Commun.* **2020**, *11* (1), 2664.

(19) Remmerswaal, W. A.; Houthuijs, K. J.; van de Ven, R.; Elferink, H.; Hansen, T.; Berden, G.; Overkleeft, H. S.; van der Marel, G. A.; Rutjes, F. P. J. T.; Filippov, D. V.; Boltje, T. J.; Martens, J.; Oomens, J.; Codée, J. D. C. Stabilization of Glucosyl Dioxolenium Ions by "Dual Participation" of the 2,2-Dimethyl-2-(*Ortho*-Nitrophenyl)Acetyl (DMNPA) Protection Group for 1,2-*Cis*-Glucosylation. *J. Org. Chem.* **2022**, *87* (14), 9139–9147.

(20) Minehan, T. G.; Kishi, Y. β-Selective C-Glycosidations: Lewis-Acid Mediated Reactions of Carbohydrates with Silyl Ketene Acetals. *Tetrahedron Lett.* **1997**, *38* (39), 6815–6818.

(21) Mayr, H.; Ofial, A. R. The Reactivity–Selectivity Principle: An Imperishable Myth in Organic Chemistry. *Angew. Chem. Int. Ed.* **2006**, *45* (12), 1844–1854.

(22) Hammett, L. P. The Effect of Structure upon the Reactions of Organic Compounds. Benzene Derivatives. *J. Am. Chem. Soc.* **1937**, *59* (1), 96–103.
(23) Gash, K. B.; Yuen, G. U. Acetolysis of Trans-2-(Tosyloxy)Cyclohexyl Substituted Benzoates. Kinetics and Oxygen-18 Studies. *J. Org. Chem.* **1969**, *34* (3), 720–724.
(24) Heuckendorff, M.; Pedersen, C. M.; Bols, M. The Influence of Neighboring Group Participation on the Hydrolysis of 2-*O*-Substituted Methyl Glucopyranosides. *Org. Lett.* **2011**, *13* (22), 5956–5959.
(25) Glaudemans, C. P. J.; Fletcher, H. G. The Methanolysis of Some D-Arabinofuranosyl Halides Having a Nonparticipating Group at Carbon 2. *J. Am. Chem. Soc.* **1965**, *87* (11), 2456–2461.
(26) Larsen, C. H.; Ridgway, B. H.; Shaw, J. T.; Woerpel, K. A. A Stereoelectronic Model To Explain the Highly Stereoselective Reactions of Nucleophiles with Five-Membered-Ring Oxocarbenium Ions. *J. Am. Chem. Soc.* **1999**, *121* (51), 12208–12209.
(27) Demkiw, K. M.; Remmerswaal, W. A.; Hansen, T.; van der Marel, G. A.; Codée, J. D. C.; Woerpel, K. A. Halogen Atom Participation in Guiding the Stereochemical Outcomes of Acetal Substitution Reactions. *Angew. Chem. Int. Ed.* **2022**, *61*, e202209401.
(28) Hagen, G.; Mayr, H. Kinetics of the Reactions of Allylsilanes, Allylgermanes, and Allylstannanes with Carbenium Ions. *J. Am. Chem. Soc.* **1991**, *113* (13), 4954–4961.
(29) A detailed examination on reaction conditions can be found in Chun, Y.; Remmerswaal, W. A.; Codée, J. D. C.; Woerpel, K. A. Neighboring-Group Participation by C-2 Acyloxy Groups: Influence of the Nucleophile and Acyl Group on the Stereochemical Outcome of Acetal Substitution Reactions. *Chem. Eur. J.* **2023**, 29, e202301894.
(30) Synthetic procedures and details of stereochemical proofs can be found in the online supporting information of: Chun, Y.; Remmerswaal, W. A.; Codée, J. D. C.; Woerpel, K. A. Neighboring-Group Participation by C-2 Acyloxy Groups: Influence of the Nucleophile and Acyl Group on the Stereochemical Outcome of Acetal Substitution Reactions. *Chem. Eur. J.* **2023**, 29, e202301894.
(31) Mayr, H.; Kempf, B.; Ofial, A. R. π-Nucleophilicity in Carbon–Carbon Bond-Forming Reactions. *Acc. Chem. Res.* **2003**, *36* (1), 66–77.
(32) Minegishi, S.; Kobayashi, S.; Mayr, H. Solvent Nucleophilicity. *J. Am. Chem. Soc.* **2004**, *126* (16), 5174–5181.
(33) Joosten, A.; Boultadakis-Arapinis, M.; Gandon, V.; Micouin, L.; Lecourt, T. Substitution of the Participating Group of Glycosyl Donors by a Halogen Atom: Influence on the Rearrangement of Transient Orthoesters Formed during Glycosylation Reactions. *J. Org. Chem.* **2017**, *82* (6), 3291–3297.
(34) Otte, D. A. L.; Borchmann, D. E.; Lin, C.; Weck, M.; Woerpel, K. A. $^{13}$C NMR Spectroscopy for the Quantitative Determination of Compound Ratios and Polymer End Groups. *Org. Lett.* **2014**, *16* (6), 1566–1569.
(35) Krumper, J. R.; Salamant, W. A.; Woerpel, K. A. Continuum of Mechanisms for Nucleophilic Substitutions of Cyclic Acetals. *Org. Lett.* **2008**, *10* (21), 4907–4910.
(36) Woods, R. J.; Andrews, C. W.; Bowen, J. P. Molecular Mechanical Investigations of the Properties of Oxocarbenium Ions. 2. Application to Glycoside Hydrolysis. *J. Am. Chem. Soc.* **1992**, *114* (3), 859–864.
(37) Krumper, J. R.; Salamant, W. A.; Woerpel, K. A. Correlations Between Nucleophilicities and Selectivities in the Substitutions of Tetrahydropyran Acetals. *J. Org. Chem.* **2009**, *74* (21), 8039–8050.
(38) Notably, a series of oxygen nucleophiles provided similar trends to the carbon nucleophiles. A detailed discussion can be found in Chun, Y.; Remmerswaal, W. A.; Codée, J. D. C.; Woerpel, K. A. Neighboring-Group Participation by C-2 Acyloxy Groups: Influence of the Nucleophile and Acyl Group on the Stereochemical Outcome of Acetal Substitution Reactions. *Chem. Eur. J.* **2023**, 29, e202301894.
(39) Chun, Y.; Remmerswaal, W. A.; Codée, J. D. C.; Woerpel, K. A. Neighboring-Group Participation by C-2 Acyloxy Groups: Influence of the Nucleophile and Acyl Group on the Stereochemical Outcome of Acetal Substitution Reactions. *Chem. – Eur. J.* **2023**, *29*, e202301894.
(40) Greis, K.; Leichnitz, S.; Kirschbaum, C.; Chang, C.-W.; Lin, M.-H.; Meijer, G.; von Helden, G.; Seeberger, P. H.; Pagel, K. The Influence of the Electron Density in Acyl Protecting Groups on the Selectivity of Galactose Formation. *J. Am. Chem. Soc.* **2022**, *144* (44), 20258–20266.
(41) Demchenko, A. V.; Rousson, E.; Boons, G.-J. Stereoselective 1,2-*c*Is-Galactosylation Assisted by Remote Neighboring Group Participation and Solvent Effects. *Tetrahedron Lett.* **1999**, *40* (36), 6523–6526.
(42) Xu, K.; Xie, D. A Computational Study of the Mechanism for the Transmetalation of 2-Trimethylstannylbuta-1,3-Diene with $SnCl_4$. *J. Org. Chem.* **2003**, *68* (7), 2673–2679.
(43) Denmark, S. E.; Wilson, Thomas.; Willson, T. M. On the Lewis-Acid-Induced Addition of Allylstannanes to Aldehydes: A Spectroscopic Investigation. *J. Am. Chem. Soc.* **1988**, *110* (3), 984–986.
(44) Neese, F. The ORCA Program System. *WIREs Comput. Mol. Sci.* **2012**, *2* (1), 73–78.
(45) Neese, F.; Wennmohs, F.; Becker, U.; Riplinger, C. The ORCA Quantum Chemistry Program Package. *J. Chem. Phys.* **2020**, *152* (22), 224108.
(46) Neese, F. Software Update: The ORCA Program System—Version 5.0. *WIREs Comput. Mol. Sci.* **2022**, *12* (5), e1606.
(47) Grimme, S.; Antony, J.; Ehrlich, S.; Krieg, H. A Consistent and Accurate Ab Initio Parametrization of Density Functional Dispersion Correction (DFT-D) for the 94 Elements H-Pu. *J. Chem. Phys.* **2010**, *132* (15), 154104.

(48) Grimme, S.; Ehrlich, S.; Goerigk, L. Effect of the Damping Function in Dispersion Corrected Density Functional Theory. *J. Comput. Chem.* **2011**, *32* (7), 1456–1465.
(49) Caldeweyher, E.; Bannwarth, C.; Grimme, S. Extension of the D3 Dispersion Coefficient Model. *J. Chem. Phys.* **2017**, *147* (3), 034112.
(50) Becke, A. D. Density-functional Thermochemistry. III. The Role of Exact Exchange. *J. Chem. Phys.* **1993**, *98* (7), 5648–5652.
(51) Lee, C.; Yang, W.; Parr, R. G. Development of the Colle-Salvetti Correlation-Energy Formula into a Functional of the Electron Density. *Phys. Rev. B Condens. Matter* **1988**, *37* (2), 785–789.
(52) Vosko, S. H.; Wilk, L.; Nusair, M. Accurate Spin-Dependent Electron Liquid Correlation Energies for Local Spin Density Calculations: A Critical Analysis. *Can. J. Phys.* **1980**, *58* (8), 1200–1211.
(53) Stephens, P. J.; Devlin, F. J.; Chabalowski, C. F.; Frisch, M. J. Ab Initio Calculation of Vibrational Absorption and Circular Dichroism Spectra Using Density Functional Force Fields. *J. Phys. Chem.* **1994**, *98* (45), 11623–11627.
(54) Weigend, F.; Ahlrichs, R. Balanced Basis Sets of Split Valence, Triple Zeta Valence and Quadruple Zeta Valence Quality for H to Rn: Design and Assessment of Accuracy. *Phys. Chem. Chem. Phys.* **2005**, *7* (18), 3297–3305.
(55) Santra, G.; Sylvetsky, N.; Martin, J. M. L. Minimally Empirical Double-Hybrid Functionals Trained against the GMTKN55 Database: revDSD-PBEP86-D4, revDOD-PBE-D4, and DOD-SCAN-D4. *J. Phys. Chem. A* **2019**, *123* (24), 5129–5143.
(56) Santra, G.; Cho, M.; Martin, J. M. L. Exploring Avenues beyond Revised DSD Functionals: I. Range Separation, with xDSD as a Special Case. *J. Phys. Chem. A* **2021**, *125* (21), 4614–4627.
(57) Remmerswaal, W. A.; Hansen, T.; Hamlin, T. A.; Codée, J. D. C. Origin of Stereoselectivity in $S_E2'$ Reactions of Six-Membered Ring Oxocarbenium Ions. *Chem. – Eur. J.* **2023**, *29* (14), e202203490.
(58) Hansen, T.; Lebedel, L.; Remmerswaal, W. A.; van der Vorm, S.; Wander, D. P. A.; Somers, M.; Overkleeft, H. S.; Filippov, D. V.; Désiré, J.; Mingot, A.; Bleriot, Y.; van der Marel, G. A.; Thibaudeau, S.; Codée, J. D. C. Defining the $S_N1$ Side of Glycosylation Reactions: Stereoselectivity of Glycopyranosyl Cations. *ACS Cent. Sci.* **2019**, *5* (5), 781–788.
(59) Elferink, H.; Remmerswaal, W. A.; Houthuijs, K. J.; Jansen, O.; Hansen, T.; Rijs, A. M.; Berden, G.; Martens, J.; Oomens, J.; Codée, J. D. C.; Boltje, T. J. Competing C-4 and C-5-Acyl Stabilization of Uronic Acid Glycosyl Cations. *Chem. – Eur. J.* **2022**, *28*, e202201724.